

Chemical Science

rsc.li/chemical-science



ISSN 2041-6539

EDGE ARTICLE

Takashi Ooi *et al.*

o-Quinone methide with overcrowded olefin component as a dehydridation catalyst under aerobic photoirradiation conditions

Cite this: *Chem. Sci.*, 2021, **12**, 2778

All publication charges for this article have been paid for by the Royal Society of Chemistry

Received 12th November 2020
Accepted 10th January 2021

DOI: 10.1039/d0sc06240e
rsc.li/chemical-science

Introduction

In contrast to the catalytic transformations that proceed through deprotonative generation of an anion as a nucleophile, alternative reactions triggered by hydride abstraction to generate a cationic intermediate as an electrophile have garnered less attention in organic chemistry, as a chemical term “dehydridation” sounds unusual. This is probably because of a deficit in effective catalysts for dehydridation, which could be ascribed to the intrinsic problems associated with the dehydridative transformations.^{1,2} While the deprotonative system commonly relies on base catalysis (proton-transfer catalysis) and involves deprotonation and protonation to complete a catalyst turnover,³ the dehydridative system generally lacks the catalyst regeneration step, rendering the development of the dehydridation catalyst difficult (Fig. 1). Mechanistically, initial dehydridation from a substrate generates a cationic intermediate and hydridated catalyst (H-Cat^-), and subsequent bond formation furnishes a cationic product precursor. The precursor is prone to liberate a cationic group (G^+), such as proton and trialkylsilylum ions, to yield a stable product rather than accepting a hydride for the catalyst regeneration. Therefore, the dehydridation catalyst often requires an independent oxidative regeneration process, in which the terminal oxidant should selectively react with H-Cat^- without degrading the

substrate. These features constitute inherent impediments to eliciting the full synthetic potential of dehydridative catalysis.⁴

In view of designing a dehydridation catalyst under these circumstances, we became interested in one of the canonical structures of *o*-quinone methide (*o*-QM), which could be regarded as a zwitterionic triarylmethilide (Scheme 1).⁵ As triarylmethilide (triarylcarbenium) ion, exemplified by tritylium ion, has been used as a powerful dehydridating reagent,⁴ we envisioned that the zwitterionic form of *o*-QM could have an ability to engage in dehydridation, being transformed to its hydrogenated (reduced) form, *o*-diarylmethyl arylhydroxide. However, although *o*-QMs undergo 1,4-addition of various nucleophiles, their capability of accepting a hydride from simple organic molecules, 1,4-reduction reactivity, remains obscure.⁶ On the other hand, *o*-diarylmethyl arylhydroxide is known to be converted to *o*-QM under mild oxidative conditions,⁷ which implies the feasibility of *in situ* regeneration of *o*-QM after dehydridation event. These characteristics of *o*-QMs and their redox behavior prompted us to explore the possibility of imparting reactivity as a dehydridation catalyst to *o*-QMs through pertinent structural modifications and optimization of

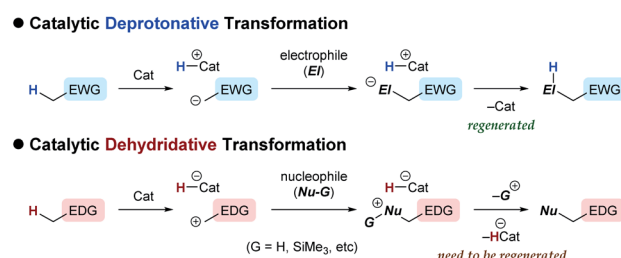


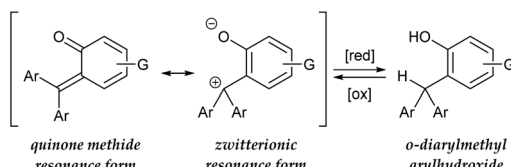
Fig. 1 General schemes of catalytic deprotonative and dehydridative transformations.

^aInstitute for Catalysis, Hokkaido University, Sapporo 001-0021, Japan

^bInstitute of Transformative Bio-Molecules (WPI-ITbM) and Department of Molecular and Macromolecular Chemistry Graduate School of Engineering, Nagoya University, Nagoya 464-8601, Japan. E-mail: tooi@chembio.nagoya-u.ac.jp

† Electronic supplementary information (ESI) available. CCDC 1993085, 1993086 and 1993087. For ESI and crystallographic data in CIF or other electronic format see DOI: 10.1039/d0sc06240e





Scheme 1 Hypothetical basis of potential hydride-abSTRACTING capability of *o*-quinone methide.

reaction conditions. Here, we report the implementation of this approach, revealing the catalytic performance of novel *o*-QM featuring an overcrowded olefinic core in the dehydridative oxidation of secondary benzyllic alcohols under aerobic photo-irradiation conditions.

Results and discussion

At the outset, we selected a representative isolable *o*-QM **1**⁸ (Fig. 2a), and evaluated its intrinsic reactivity toward an organic reductant, 2-phenylbenzothiazoline,⁹ in CDCl_3 by ^1H NMR (400 MHz) monitoring experiment, which showed that conversion of **1** to the reduced form **1-H₂** *via* 1,4-reduction did not occur (Fig. 3a). We inferred that the observed low reactivity could be ascribed to the insufficient contribution of the zwitterionic canonical form to the resonance structures of **1**. To increase the zwitterionic character of *o*-QM, we devised an *o*-QM **2H** featuring 10,10-dimethyl-9(*10H*)-anthracenylidene framework with expectation that **2H** would be compelled to form a twisted

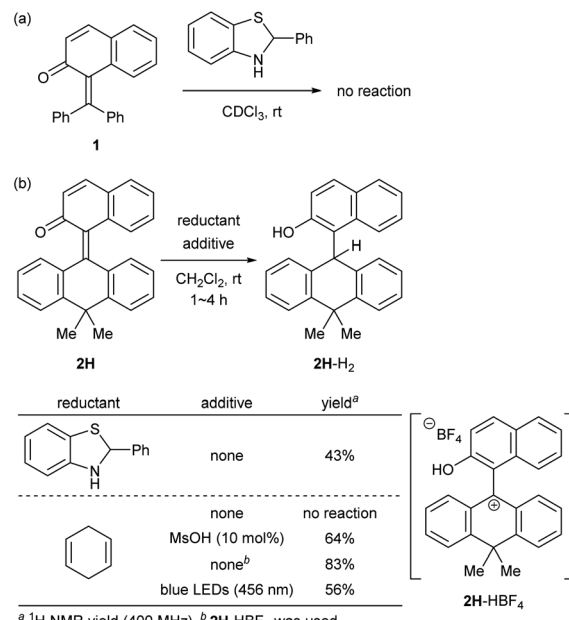


Fig. 3 Reduction of *o*-QM **1** (a) and **2H** (b).

structure due to the steric repulsion between the substituents on the olefinic carbons at the fjord region. However, X-ray diffraction analysis of an orange crystal of **2H** revealed its distorted but non-twisted (*anti*-folded) three-dimensional structure having a nearly identical α,β -unsaturated core to that of **1** (Fig. 2b). The burden of the distortion is mainly localized on the

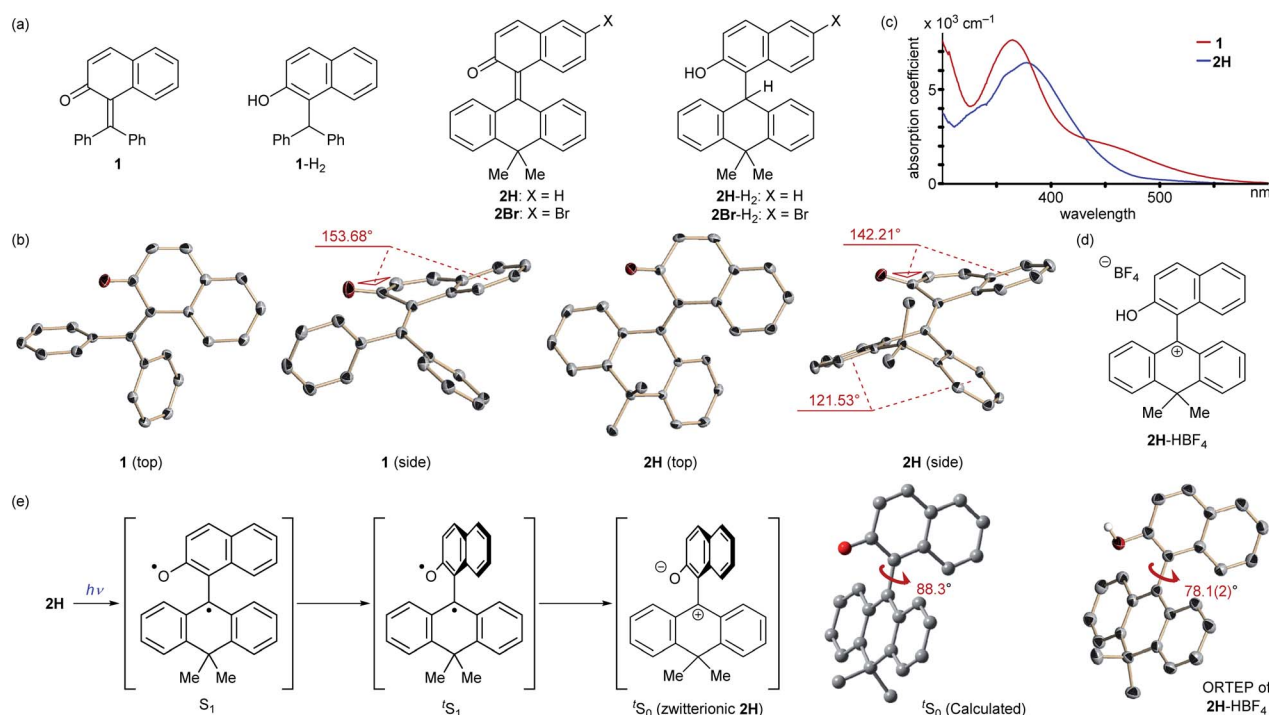


Fig. 2 (a) Molecular structures of *o*-QMs and their reduced forms. (b) ORTEP diagrams of *o*-QMs. (c) UV spectra of *o*-QMs. (d) Structure and ORTEP diagram of protonated *o*-QM, **2H-HBF₄** (BF_4^- was omitted for clarity). (e) Expected molecular motion of **2H** upon photoexcitation and calculated structure of $'\text{S}_0$ (calculated) ORTEP of **2H-HBF₄**.



ring systems. Specifically, the mean plane dihedral angle of the benzocyclohexadienone subunit of **2H** (142.21°) is markedly smaller than that of **1** (153.68°), and the dihydroanthracene subunit is also significantly bent (121.53°). *In silico* structural optimization of **2H** and **1** using density functional theory (DFT) calculations (SMD(CH_2Cl_2)-CAMB3LYP/6-31+G(d) level)¹⁰ derived nearly identical structures to those obtained from the X-ray analysis, suggesting that the observed skeletal distortion was not affected by the crystal packing force (see ESI[†]). In addition, a comparison of the maximum absorption wavelengths of **2H** (381 nm) with that of **1** (363 nm) supports a similar effective conjugation length (α,β -unsaturated character) (Fig. 2c). These observations implied a negligible difference in the cationic character of their benzylic carbons. However, **2H** reacted with 2-phenylbenzothiazoline with higher efficiency to give the reduced form **2H-H₂** at ambient temperature (43%), suggesting the enhanced cationicity (Fig. 3b). Although **2H** did not undergo 1,4-reduction with less reactive cyclohexa-1,4-diene as a hydride donor, its dehydratation activity could be enhanced by adding an acidic additive to effectively increase the participation of the zwitterionic structure as its protonated, carbocationic form. For instance, the reaction of **2H** with cyclohexa-1,4-diene proceeded smoothly in the presence of 10 mol% of methanesulfonic acid (MsOH) to afford **2H-H₂** in 64% yield. Protonation of the carbonyl oxygen of *o*-QM induces the generation of the protonated form of the zwitterionic resonance structure of **2H**, **2H-HOMs**, as evident from the indicative change in solution color from pale yellow to deep red. For precise structural elucidation of the protonated form of **2H**, **2H-HBF₄** was separately prepared by the treatment of **2H-H₂O** with HBF₄ in toluene. The subsequent recrystallization from the hexane/ CH_2Cl_2 solvent system gave deep red crystals, which were subjected to X-ray diffraction analysis. As shown in Fig. 2d, 2-naphthol and dihydroanthracene subunits connected perpendicularly (torsion angle: 78.1°), and the benzylic carbon of the connecting bond adopted an almost complete sp^2 -hybridized planar structure (sum of the angles: 360°), accounting for its cationic character. Notably, the reduction of **2H-HBF₄** to **2H-H₂** with cyclohexa-1,4-diene was even faster (83%), demonstrating its high reactivity. These observations corroborate the correlation between the cationicity of the benzylic carbon atom of *o*-QM **2H** and its dehydratation activity.

Having verified the structure–activity relationship of *o*-QM **2H** in the reduction with the hydride donors, we were intrigued with the possibility of increasing the reactivity of **2H** by other means, preferably by taking advantage of its inherent structural attributes, without the addition of acidic additives. Toward this end, we paid our attention to the push–pull-type structure of the tetrasubstituted olefinic component of **2H** and envisaged that its local excitation by photoirradiation would cause twisting around the C–C axis at the singlet excited state (S_1) of the folded conformer to give stabilized twisted S_1 ($'S_1$), in analogy with the behavior of the overcrowded ethylenes (Fig. 2e).¹¹ Further relaxation with preservation of the twisted structure furnishes ground-state intermediate $'S_0$ of distinct zwitterionic character, which would exert enhanced dehydratation activity. This

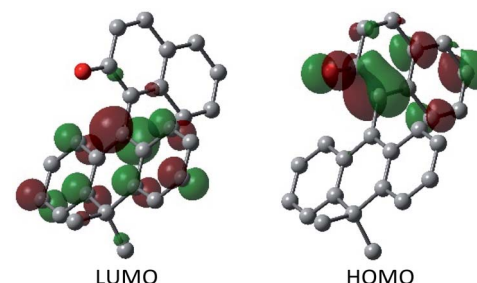
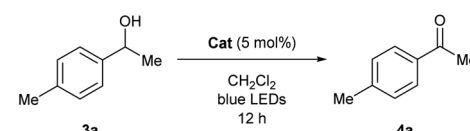


Fig. 4 Molecular orbital of $'S_0$ of **2H**.

hypothesis was substantiated by attempting the reaction of **2H** with cyclohexa-1,4-diene in CH_2Cl_2 under irradiation with blue LEDs (456 nm), which exhibited smooth conversion into **2H-H₂** (56% for 1 h, Fig. 3b). To obtain support for the origin of the increased hydride-abstrating ability of **2H**, we calculated the structure of $'S_0$ at the SMD(CH_2Cl_2)-TD-CAMB3LYP/6-31+G(d) level and confirmed its similarity to the structure of **2H-HBF₄** in accordance with the presumed predominant contribution of the zwitterionic form (Fig. 2d *vs.* 2e). Molecular orbital of $'S_0$ revealed intramolecular charge separation and the largest orbital lobe in LUMO of the resultant zwitterionic structure resided at the benzylic carbon in good agreement with its expected carbocationic character (Fig. 4).

To experimentally explore the feasibility of the dehydrative catalysis of *o*-QMs, we chose the oxidation of benzylic secondary alcohols as a model reaction system. Prior to assessing the viability of the regeneration of *o*-QM with various oxidants, we sought to evaluate the intrinsic reactivity of **2H** as a dehydratation catalyst with 1-(4-methylphenyl)ethyl alcohol (**3a**) as a representative substrate (Table 1). Thus, **3a** was treated with each 5 mol% of **2H** and the co-catalyst MsOH in CH_2Cl_2 at ambient temperature for 12 h, which produced 4-

Table 1 Optimization^a



Entry	Catalyst	Yield ^b (%)	Note
1	2H	4	MsOH (5 mol%) without photoirradiation
2	2H	17	Under Ar
3	2H	51	Under air
4	2H	59	Under O ₂
5	2H	4	Under Ar (degassed)
6	2H-H₂	76	Under O ₂
7	2Br-H₂	97	Under O ₂
8	1	8	Under O ₂

^a Unless otherwise noted, reaction was performed with 0.1 mmol of **3a** in the presence of 5 mol% of catalyst in CH_2Cl_2 under blue LEDs irradiation (456 nm) at ambient temperature for 12 h. ^b ¹H NMR yield (400 MHz) determined by trimethylsilylbenzene as the internal standard.

methylacetophenone (**4a**) in 4% ^1H NMR yield (400 MHz, trimethylsilylbenzene as the internal standard), an amount less than the loading of **2H** (entry 1). Considering the beneficial effect of photoirradiation on the reactivity of **2H**, we also conducted the reaction with irradiation of blue LEDs (456 nm) in the absence of MsOH under otherwise similar conditions, which exhibited a higher conversion to afford **4a** in 17% yield (entry 2). While this unexpected outcome suggested the possibility of regenerating **2H** with photoirradiation, close examination of the reaction conditions revealed that traces of O_2 acted as an oxidant to regenerate **2H** under light irradiation. Indeed, performing the reaction under air and O_2 atmospheres further improved conversion to 51% and 59%, respectively, whereas only a trace amount of **4a** was detected under a thoroughly inert atmosphere (entries 3–5). These profiles led us to attempt the reaction with the reduced form **2H-H₂** as a pre-catalyst, assuming that active catalyst **2H** could be generated *in situ* under aerobic photoirradiation conditions (entry 6). The observed high conversion of **3a** validated the hypothesis and the operation of the dehydrative catalysis of **2H** in this oxidation. This finding allowed us to continue further investigation with the use of more stable and easy-to-handle **2H-H₂** as a pre-catalyst, and we found that introduction of a bromo functionality to the 6-position of the 2-naphthol subunit (**2Br-H₂**) delivered a critical enhancement in the catalytic activity, enabling a complete conversion of **3a** within 12 h (entry 7). It should be noted that the importance of the overcrowded alkene component of **2H** for exerting efficient dehydrative catalysis was confirmed by comparing the reactivity with that of **1** (entry 8).

With the optimized conditions in hand, we turned our attention to examine the substrate scope of the dehydrative catalysis (Table 2). Generally, 5 mol% of **2Br-H₂** was sufficient for smooth conversion of alcohols **3** to afford the corresponding ketones **4** in high chemical yield. Incorporation of various substituents of different electronic properties to an arbitrary position of the aromatic nuclei was tolerated (entries 1–10). The alkyl substituent on the hydroxy-bearing carbon could also be varied and not only linear but also branched chains were well accommodated (entries 11–15). As demonstrated in the reaction with a diol, chemoselective oxidation of benzylic alcohols over aliphatic alcohols was feasible (entry 16).¹² In addition, scalability of this protocol was confirmed with **3a** as a substrate (entry 17).

To gain further insight into the reaction mechanism, we simulated the molecular motion of the postulated excitation process of **2H** using time-dependent density functional theory (TD-DFT) calculations (SMD(CH_2Cl_2)-TD-CAMB3LYP/6-31+G(d) level). As illustrated in Fig. 5, the calculated energy difference between the folded S_1 and $'\text{S}_1$ ($\Delta E = 2.15$ eV) signified that photoexcitation of **2H** to S_1 and spontaneous unfolding furnishes $'\text{S}_1$. The subsequent rapid relaxation to the ground-state zwitterionic intermediate $'\text{S}_0$ may well occur owing to the small energy gap ($\Delta E = 0.43$ eV), while this process was estimated to be a forbidden transition. Further simulation of the folding pathway from $'\text{S}_0$ to S_0 to estimate the lifetime of $'\text{S}_0$ uncovered the intervention of a two-step transition process

Table 2 Substrate generality^a

Entry	Ar	R	Yield ^b (%)
1	4-CF ₃ C ₆ H ₄	Me	85
2	4-NCC ₆ H ₄	Me	94
3	4-ClC ₆ H ₄	Me	84
4	4-BrC ₆ H ₄	Me	97
5	C ₆ H ₅	Me	90
6	3-ClC ₆ H ₄	Me	86
7	3-MeC ₆ H ₄	Me	86
8	3-MeOC ₆ H ₄	Me	95
9	2-ClC ₆ H ₄	Me	89
10	2-MeC ₆ H ₄	Me	72
11	C ₆ H ₅	Et	98
12	C ₆ H ₅	ⁿ Pr	99
13	C ₆ H ₅	ⁱ Bu	84
14	C ₆ H ₅	ⁱ Pr	87
15	C ₆ H ₅	^c Hex	94
16	C ₆ H ₅	(CH ₂) ₂ OH	77
17 ^c	4-MeC ₆ H ₄	Me	74

^a Unless otherwise noted, reaction was conducted on 0.1 mmol scale with 5 mol% of **2Br-H₂** in CH_2Cl_2 under photoirradiation (456 nm) for 12 h. ^b Isolated yield was indicated. ^c 5 mmol scale reaction.

(Fig. 6). Following the relaxation from $'\text{S}_1$, $'\text{S}_0$ spontaneously undergoes conformational change to give thermodynamically more stable **int1**. Then, increase in the double-bond character of the bridging C–C bond with concurrent bending of the

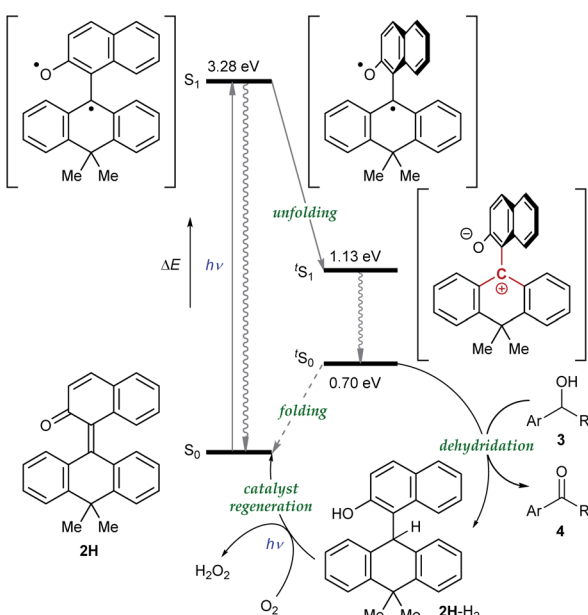


Fig. 5 Plausible mechanism.



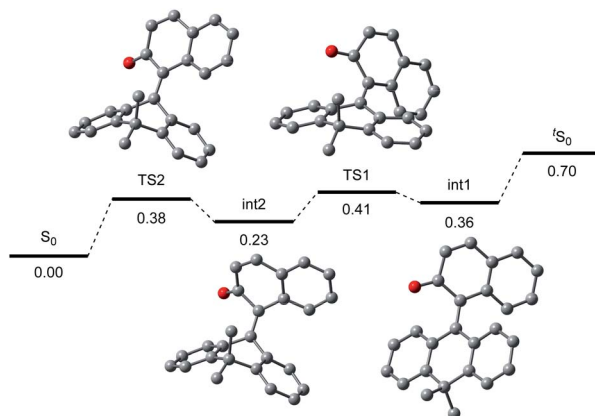


Fig. 6 Folding process from tS_0 (upper right) to S_0 (lower left).

dihydroanthracene subunit along the C9–C10 axis affords int2 *via* TS2. Subsequent rotation around the bridging C–C bond eventually forms S_0 *via* TS1. These computational analyses imply that int1 would have a certain lifetime, although both of the two energetic barriers of the folding process are very small. Accordingly, the triarylmethilide moiety of tS_0 would engage in dehydridation from the methine carbon of alcohol 3 to give the corresponding ketone 4 with concomitant generation of $2H\text{-H}_2$. During this process, the aryloxide moiety of tS_0 would simultaneously accept a proton from the hydroxy functionality of 3. The regeneration of $2H$ from $2H\text{-H}_2$ is facilitated likely by active oxygen species, such as singlet oxygen or superoxide, generated through excitation of O_2 by sensitization with the 2-naphthol subunit of the catalyst, as confirmed by the detection of H_2O_2 in the reaction mixture (see ESI†).^{13–15} UV-vis spectrum of $2H\text{-H}_2$ indicated that its absorption terminus reaches 470 nm and thus, $2H\text{-H}_2$ could be excited by irradiation of blue LEDs (Fig. S2†). The estimated energy of $2H\text{-H}_2$ at the excited state was 2.17 eV, which is sufficient to activate the ground-state triplet O_2 , allowing the regeneration of $2H$ through rapid abstraction of the neighboring benzylic hydrogen by the resulting activated O_2 . Although the TD-DFT analysis also suggested the feasibility of an alternative process involving an electron-donor-acceptor (EDA) complex of $2H\text{-H}_2$ and O_2 followed by its photoexcitation, careful examination of the UV-vis spectroscopy of $2H\text{-H}_2$ under Ar and O_2 atmospheres showed no evidence of the formation of EDA complex.

Conclusions

We have demonstrated the feasibility of eliciting the latent reactivity of *o*-QMs as a dehydridation catalyst. The introduction of an overcrowded olefinic framework is a key for enhancing the contribution of the zwitterionic resonance form of *o*-QM and its dehydridation activity can be fully realized by photoexcitation. This unique property of the novel *o*-QM is exploited to establish dehydridative catalysis in the oxidation of benzylic secondary alcohols under aerobic photoirradiation conditions, where the ground-state zwitterionic intermediate acts as an actual reactive species and the catalyst is regenerated by either singlet oxygen

or superoxide as supported by experimental and theoretical analyses. We anticipate that the present study stimulates further research endeavor for exploring synthetic potential of dehydridative catalysis.

Conflicts of interest

There are no conflicts to declare.

Acknowledgements

Financial support was provided by a Grant-in-Aid for Scientific Research on Innovative Areas “Hybrid Catalysis” (No. 17H06444, to TO), and Grants of JSPS for Scientific Research. This work was also supported by Program for Leading Graduate Schools “Integrative Graduate Education and Research Program in Green Natural Sciences” in Nagoya University and WISE Program (Doctoral Program for World-leading Innovative & Smart Education) “Graduate Program of Transformative Chem-Bio Research” in Nagoya University. We appreciate Prof. Daisuke Yokogawa (Univ. of Tokyo) and Prof. Takeshi Yanai (Nagoya Univ.) for insightful discussion on the theoretical analysis.

Notes and references

- (a) R. R. Naredla and D. A. Klumpp, *Chem. Rev.*, 2013, **113**, 6905; (b) A. E. Wendlandt and S. S. Stahl, *Angew. Chem., Int. Ed.*, 2015, **54**, 14638.
- J.-J. Tian, N.-N. Zeng, N. Liu, X.-S. Tu and X.-C. Wang, *ACS Catal.*, 2019, **9**, 295.
- N. Kumagai and M. Shibasaki, *Angew. Chem., Int. Ed.*, 2011, **50**, 4760.
- (a) M. E. Jung and L. M. Speltz, *J. Am. Chem. Soc.*, 1976, **98**, 7882; (b) J. M. Gil-Negrete, J. P. Sestelo and L. A. Sarandeses, *J. Org. Chem.*, 2019, **84**, 9778; (c) W. Chen, Z. Xie, H. Zheng, H. Lou and L. Liu, *Org. Lett.*, 2014, **16**, 5988; (d) M. E. Jung, *J. Org. Chem.*, 1976, **41**, 1479; (e) M. E. Jung and R. W. Brown, *Tetrahedron Lett.*, 1978, **31**, 2771; (f) M. E. Jung, Y.-G. Pan, M. W. Rathke, D. F. Sullivan and R. P. Woodbury, *J. Org. Chem.*, 1977, **42**, 3961; (g) M. Wan, Z. Meng, H. Lou and L. Liu, *Angew. Chem., Int. Ed.*, 2014, **53**, 13845; (h) X. Liu, Z. Meng, C. Li, H. Lou and L. Liu, *Angew. Chem., Int. Ed.*, 2015, **54**, 6012; (i) T. Katsina, L. Clavier, J.-F. Giffard, N. M. Portela da Silva, J. Fournier, R. Tamion, C. Copin, S. Arseniyadis and A. Jean, *Org. Process Res. Dev.*, 2020, **24**, 856.
- (a) H. Sugimoto, S. Nakamura and T. Ohwada, *Adv. Synth. Catal.*, 2007, **349**, 669; (b) T. P. Pathak and M. S. Sigman, *J. Org. Chem.*, 2011, **76**, 9210; (c) M. M. Toteva and J. P. Richard, in *Advances in Physical Organic Chemistry*, ed. J. P. Richard, Elsevier, 2011, vol. 45, pp. 39–91; (d) D. Škalamera, K. Mlinarić-Majerski, I. M. Kleiner, M. Kralj, J. Oake, P. Wan, C. Bohne and N. Basarić, *J. Org. Chem.*, 2017, **82**, 6006.
- (a) R. Chen, Y. Liu and S. Cui, *Chem. Commun.*, 2018, **54**, 11753; (b) M.-M. Chu, S.-S. Qi, W.-Z. Ju, Y.-F. Wang,



X.-Y. Chen, D.-Q. Xu and Z.-Y. Xu, *Org. Chem. Front.*, 2019, **6**, 1140 and references therein.

7 T. Inoue, S. Inoue and K. Sato, *Bull. Chem. Soc. Jpn.*, 1990, **63**, 1062.

8 T. W. Lewis, E. N. Duesler, R. B. Kress, D. Y. Curtin and I. C. Paul, *J. Am. Chem. Soc.*, 1980, **102**, 4659.

9 (a) H. Chikashita, M. Miyazaki and K. Itoh, *Synthesis*, 1984, 308; (b) H. Chikashita, M. Miyazaki and K. Itoh, *J. Chem. Soc., Perkin Trans. 1*, 1987, 699; (c) C. Zhu, K. Saito, M. Yamanaka and T. Akiyama, *Acc. Chem. Res.*, 2015, **48**, 388.

10 (a) T. Yanai, D. P. Tew and N. C. Handy, *Chem. Phys. Lett.*, 2004, **393**, 51; (b) M. J. Frisch, *et al.*, *Gaussian 09, Revision D.01*, Gaussian, Inc., Wallingford, CT, 2009; (c) A. V. Marenich, C. J. Cramer and D. G. Truhlar, *J. Phys. Chem. B*, 2009, **113**, 6378.

11 T. Nishiuchi, R. Ito, E. Stratmann and T. Kubo, *J. Org. Chem.*, 2020, **85**, 179.

12 Under the present reaction conditions, oxidation of aliphatic primary and secondary alcohols hardly proceeded (Ph(CH₂)₃OH: <5%, cyclohexanol: 5%). In the case of allylic and propargylic alcohols, unavoidable side reactions afforded complex mixtures.

13 (a) W. M. Draper and D. G. Crosby, *J. Agric. Food Chem.*, 1983, **31**, 734; (b) M. Hayyan, M. Ali Hashim and I. M. AlNashef, *Chem. Rev.*, 2016, **116**, 3029.

14 (a) C. Matsubara, N. Kawamoto and K. Takamura, *Analyst*, 1992, **117**, 1781; (b) D. Uraguchi, M. Torii and T. Ooi, *ACS Catal.*, 2017, **7**, 2765.

15 Although singlet oxygen has been known to directly oxidize benzylic alcohols in polar solvent,¹⁶ the oxidation did not occur in the presence of methylene blue as a catalytic sensitizer in CH₂Cl₂ under blue LED irradiation.

16 (a) Y.-Z. Chen, Z. U. Wang, H. Wang, J. Lu, S.-H. Yu and H.-L. Jiang, *J. Am. Chem. Soc.*, 2017, **139**, 2035; (b) N. F. Nikitas, D. I. Tzaras, I. Triandafillidi and C. G. Kokotos, *Green Chem.*, 2020, **22**, 471.

